

IGC Newsletter

ISSN 0972-5741

Volume 104 April 2015



DIAMOND JUBILEE YEAR
60
Glorious Years
1954 - 2014

Celebrating the spirit of Diamond Jubilee Year: The Department of Atomic Energy Tableau in the 66th Republic Day Parade at New Delhi

INDIRA GANDHI CENTRE FOR ATOMIC RESEARCH
<http://www.igcar.gov.in/lis/nl104/igc104.pdf>



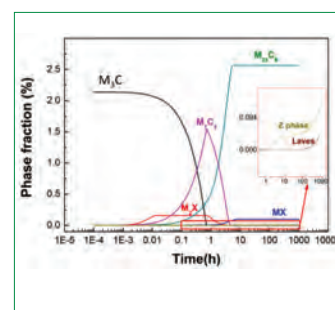
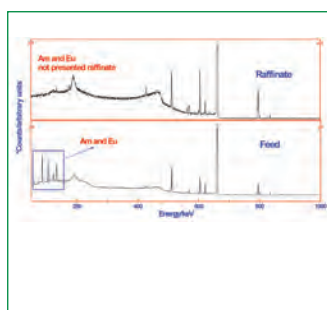
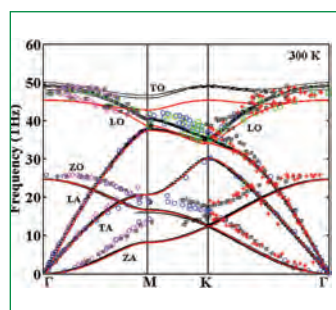
Atoms in the Service of the Nation

Celebrating its diamond jubilee year, the Department of Atomic Energy (DAE) portrays in its tableau, its expertise in harnessing the tremendous potential of the atom for the benefit of the society. The tableau is led by a white dove atop an atomic orbital symbolizing the conviction of the nation in spreading the message 'Atoms for Peace'. It also pays homage to the visionary Dr. Homi Jehangir Bhabha, founding father of the Indian Nuclear Programme. The trailer portion of the tableau is conceptually divided into three parts depicting peace, progress and prosperity, vis-a-vis the service deliverables of the Department. The first part symbolizes progress in the field of medical technology depicting the indigenously developed 'Bhabhatron' machine, used in radiotherapy and delivering affordable health care. The colourful flora, following it, showcases prosperity in food and agriculture through mutation breeding technology to provide disease-resistant and high yielding seeds and food irradiation techniques that increase the shelf life of the produce. Lastly, standing tall, the indigenous Nuclear Reactor highlights the advantage of nuclear energy to provide an unlimited supply of clean and green energy for the sustained progress of the nation.

Department of Atomic Energy

CONTENTS

Editorial Note	ii
Technical Articles	
• Development of Handheld Wireless Network Analyzers	1
• Research and Development relating to Minor Actinide Partitioning	4
 Young Officer's Forum	
• A Spectral Energy Density Based Method to Understand the Temperature Dependent Phonon Frequencies in Materials	6
 Young Researcher's Forum	
• Phase Transformations and Microstructural Evolution in 9Cr Reduced Activation Ferritic/Martensitic Steels	10
 Conference and Meeting Highlights	
• Orientation Programme for Young Officers	13
• 11 th CEA-IGCAR Annual Meeting on Liquid Metal Fast Breeder Reactor Safety	14
• Diamond Jubilee Celebrations of the Department of Atomic Energy at Kalpakkam	15
 Visit of Dignitaries	 16
 Awards & Honours	 19



From the Editor

Dear Reader

It is my pleasant privilege to forward a copy of the latest issue of IGC Newsletter (Volume 104, April 2015, issue) for your perusal.

In the first technical article Smt. Jemimah Ebenezer & colleagues have shared their experience in development of handheld wireless network analyzers for radiation monitoring network. The hardware of the tool has been designed and developed using Zigbee Sniffer. Shri K. A. Venkatesan has demonstrated the separation of lanthanides from actinides using CHON based ligand soluble in nuclear diluents with Fast Breeder Reactor waste. He has also derived a flow sheet for partitioning minor actinides from fast reactor, high-active waste solution using TRUEX solvent and explored a novel approach namely single cycle method for minor actinide partitioning using completely incinerable reagents.

Shri P. Anees has developed a spectral energy density based formalism to enumerate the temperature dependence of the phonon frequencies, dispersion and coupling of normal modes of vibration in crystal by carrying out lattice and molecular dynamic calculations which is highlighted in young officer's forum

The young researcher's forum in this issue features an article by Dr. Ravikiran on phase transformation and microstructural evolution studies on 9Cr-Reduced Activation Ferritic/Martensitic steels with varying tungsten and tantalum content.

This Newsletter carries reports on Orientation Programme for Young Officers and 11th CEA-IGCAR Annual Meeting on Liquid Metal Fast Breeder Reactor Safety.

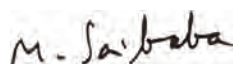
We had distinguished visitors to our Centre in the last quarter including, Dr. R. Muralidharan, Dr. Baldev Raj, Prof. Ashok Jhunjhunwala and Shri S. S. Bajaj.

We are happy to share with you the awards, honours and distinctions earned by our colleagues.

We look forward to your comments, continued guidance and support.

With my best wishes and personal regards,

Yours sincerely,



(M. Sai Baba)

Chairman, Editorial Committee, IGC Newsletter

&

Associate Director, Resources Management Group

Development of Handheld Wireless Network Analyzers

Wireless sensor networking technology is emerging as a game-changer in the field of sensing. The ease of deployment, auto-configurability and flexibility are the superior qualities of Wireless sensor network to get better acceptability in industries. Wireless sensor network comprises of multiple sensor nodes to sense the parameter to be monitored, router nodes to forward the data and base station node to get connected to a computer for live display and further processing. These nodes has been developed in-house for deploying them in applications related to nuclear facilities. Wireless sensor networking has been established in IGCAR at FBTR, RCL, INSOT, SADHANA Facility and Computer Centre. These networks are for monitoring / measuring process parameters and established for indoor deployment.

During development and deployment of wireless sensor networks, the need for handheld network analyzer tools was realized. These tools are helpful during software development phase to assist in network design and during deployment phase for assessment of development environment and traffic analysis, which in turn helps in determination of node placement.

ZigBee Sniffer

The hardware is designed and developed as 802.15.4/ Zigbee sniffer which will work along with laptop PC. This sniffer would be used in promiscuous mode to capture on-air traffic and could be used to measure the signal strength in any one of the channels of IEEE 802.15.4. (It has 16 channels in 2.4 GHz). This sniffer board has LPC1768 microcontroller and AT86RF231 wireless transceiver. This board is connected to the PC via USB interface. Block diagram for sniffer board has been shown in Figure 1.

Sniffer firmware has been developed in-house by 802.15.4 MAC stack and USB HID firmware has been developed using Keil's RL-ARM library. Input and output report size of 128 bytes has been

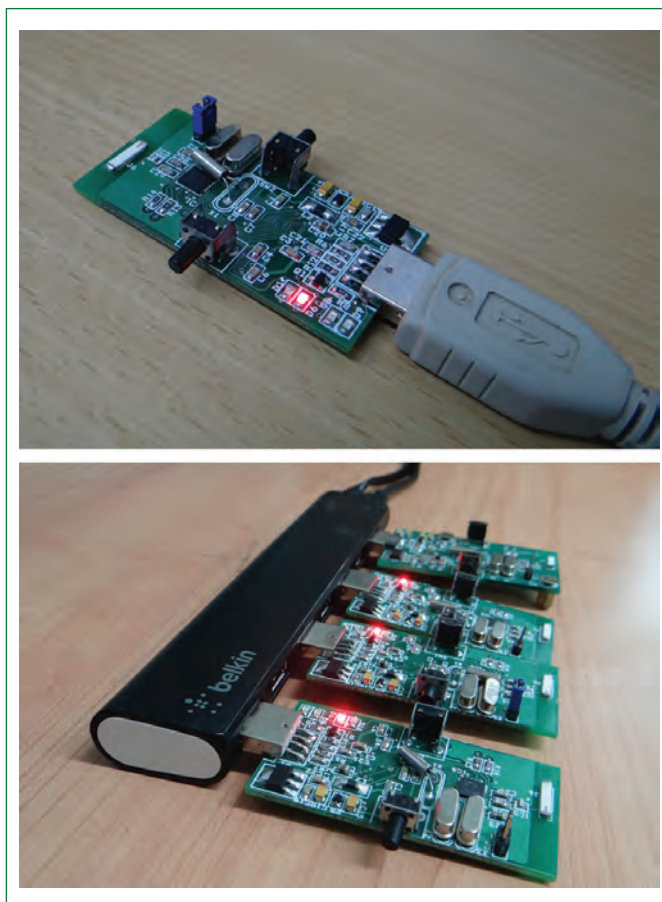


Figure 2: Zigbee sniffer and multi channel sniffer

selected, which can be used to send 127 byte 802.15.4 packets.

To provide flexibility to the administrator while working in channel hopping networks, the multichannel sniffer is needed. In a multi channel setup, multiple single channel sniffers tuned to different frequencies are connected to laptop via USB hub (Figure 2).

Based on application Zigbee sniffer can be used in two capacities: packet analyzer and spectrum analyzer.

Packet Analyzer

Packet analyzer is an important tool that can intercept the traffic passing over a digital network or part of a network. In wireless sensor networking, packet analyzer is useful during the deployment phase to analyze different network scenarios and traffic monitoring. It is useful for protocol debugging in development phase.

In this implementation, wire shark is used for packet analysis. Application corresponding to sniffer device has been written in C#. This application has three components:

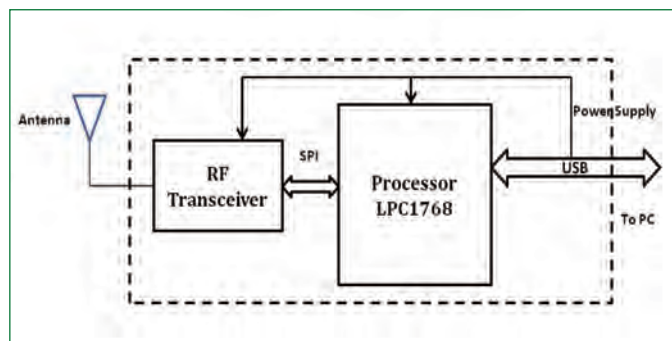


Figure 1: Block diagram of in-house developed wireless sniffer

1. Sniffer Device Driver: Corresponding USB HID plug and play driver for sniffer has been developed using .net API and tested. This driver is then modified to extend the support to multiple sniffer devices. Currently, this program can support maximum of 8 sniffers, which can be tuned to different 802.15.4 channels.

2. Sniffer Device Operation: API interface has been devised to control the operation of sniffers. This supports channel selection, starting and stopping the sniffer device and sniffed packet collection. Corresponding functionalities have been implemented in Sniffer firmware and host application.

3. Wireshark Feeding: To input the data to Wireshark, “named pipe” method has been used. Named pipe is an extension of pipe concept and is one of the methods for Inter-Process Communication (IPC). Pipes allow separate processes to communicate without designing explicitly to work together. Sniffed packets sent to the named pipes are received by Wireshark. Wireshark uses libpcap for packet capture; appropriate headers have to be added to the received data packets.

Wireshark contains different frame dissectors for different protocols. For multichannel setup, to distinguish between packet received in different frequencies, 'channel number' field has been added to the packet structure. Hence in Wireshark, the packet dissector for IEEE802.15.4 has been modified and recompiled. Currently, dissector for IEEE 802.15.4e TSCH is being developed.

Spectrum Analyzer

Spectrum analyzer is used to measure Received Signal Strength Indicator (RSSI) in any particular channel. Based on the measured RSSI value, the electromagnetic compatibility (i.e. presence of interference and other cohabitating network) of the area of interest could be determined. This utility of Zigbee sniffer is being used for site survey during pre-deployment phase and for determining the router location during the commissioning phase of wireless sensor network. Sniffer firmware for continuous RSSI measurement has been developed to find interferer. Figure 3 shows the screenshot of application for instantaneous RSSI measurement.

When used in conjunction, these tools are useful in trouble shooting the problem which can arise during development and deployment.

Handheld Solution

Sniffer tools are used along with laptop with application software developed for the same. But due to scope and deployment space of wireless sensor networking, it has been decided to develop portable solutions so that analysis of operational states and behavior of wireless sensor network could also be done at multiple locations simultaneously. Two different platforms- Neo Freerunner and Android based tablet have been used to develop these solutions.

Neo Freerunner Based Development

The Neo FreeRunner (Figure 4) is an open source smartphone that



Figure 3: Application for spectrum analyzer

is developed by the Openmoko project. Since the design of this device is open source, various ports of different operating systems are available. Some of these are OpenMoko, qtMoko, SHR, Inferno, OpenWrt, Replicant and Debian. Zigbee sniffer can be connected with this handheld device and used as network analyzer. Since Zigbee sniffer does not contain any power source, power has to be drawn from the handheld device via USB. Neo Freerunner contains USB-OHCI (Open Host Controller Interface) Chip; hence it has been used as a USB host to supply power to extenders. SHROS has been used for development, because of its active toolchain support.

SHR OS supports Vala language for developing applications. It has resemblance to and yet powerful than C language. Vala program has been developed to identify extender device as USB HID module and successfully established data communication between the Neo FreeRunner device and the extender device. Further the program has been extended to parse the data being sniffed by the extender device according to ZigBee protocol. The application is capable of identifying every ZigBee packet as data, command,



Figure 4: Neo Freerunner with wireless packet structure display

ID	TYPE	Src	Dst	Nwk Src	Nwk Dst	Length	LQI	RSSI
0.803	ROUTE_REQ	0x4B5E	0x4FFF	0x4B5E	0x4FFC	33	-4	-99dBm
0.804	APS_DATA	0x5F8D	0x0	0x5F8D	0x0	53	-1	-54dBm
0.805	ACK	-	-	-	-	5	-1	-40dBm
0.806	APS_ACK	0x0	0x5F8D	0x0	0x5F8D	43	-1	-40dBm
0.807	ACK	-	-	-	-	5	-1	-54dBm
0.808	LINK_STATUS	0x7122	0x4FFF	0x7122	0x4FFC	59	-1	-54dBm
0.809	APS_DATA	0x1425	0x0	0x1425	0x0	53	-1	-54dBm
0.810	ACK	-	-	-	-	5	-4	-39dBm
0.811	APS_ACK	0x0	0x1425	0x0	0x1425	43	-1	-39dBm
0.812	ACK	-	-	-	-	5	-1	-54dBm
0.813	APS_DATA	0x9AEC	0x0	0x9AEC	0x0	53	-1	-46dBm
0.814	ACK	-	-	-	-	5	-1	-40dBm
0.815	APS_ACK	0x0	0x9AEC	0x0	0x9AEC	43	-28	-40dBm
0.816	ACK	-	-	-	-	5	-1	-46dBm
0.817	UNKNOWN_LHWK	0x2	0x1	-	-	43	-1	-79dBm
0.818	APS_DATA	0x1	0x2	0x8CB2	0x0	19	-4	-58dBm

Figure 5: Application developed in android tablet

acknowledgement or broadcast packets. But from the point of view of managing a wireless network and also considering the width of the display of a handheld terminal, the MAC addresses, network source address and the data part of the sniffed ZigBee packet is displayed.

Android Based Development

Android application has been developed for 802.15.4/Zigbee packet sniffing. This development includes USB HID driver development for sniffer device, packet parser development and SQLite based database design for packet storage. Application layer and network layer parsing for different frame identification, session management capability and LQI/RSSI values have been incorporated with this application. It has been installed in a tablet and used as a handheld device as shown in Figure 5.

These tools are extremely useful during site surveys and deployment phase of outdoor WSN deployment for radiation monitoring network from Main gate to FBTR. They are also being used as silent observers to gather network data for post site survey and offline analysis. In future, these devices will be used as trusted devices so that it can be used to distribute security keys to view and control on-the-fly network health parameters and for calibration, configuration, maintenance and upgradation.

Reported by

Jemimah Ebenezer & colleagues, Computer Division, Electronics, Instrumentation and Radiological Safety Group

Research and Development relating to Minor Actinide Partitioning

The High level liquid waste (HLLW) is a complex mixture of several elements such as minor actinides, lanthanides, other fission products, corrosion products arising from structural materials and the additives etc., present in the dissolver solution of 3-4 M nitric acid medium. Among the various elements present in HLLW, the radiotoxicity is essentially contributed by the long-lived minor actinides such as ^{237}Np , ^{241}Am , ^{243}Am , ^{244}Cm , ^{245}Cm , ^{243}Cm and fission products such as ^{99}Tc , ^{107}Pd , ^{93}Zr , ^{129}I , ^{135}Cs , ^{137}Cs and ^{90}Sr .

Partitioning (P) of the long-lived isotopes followed by transmutation (T) of them into stable or short-lived products reduces the radiotoxicity of HLLW to a significant extent. Partitioning of trivalent minor actinides from HLLW involves a complex chemistry. The stable oxidation state of transplutonium actinides (Am and Cm) is +3. The concentration level of these actinides (~ 20 ppm) is very small in comparison to the fission product lanthanides (Ln) existing in significant concentrations (~3000 ppm). Close similarity in the chemical and extractive properties of these lanthanides (Ln(III)) with trivalent actinides (An(III)), poses challenge in achieving efficient separation of them. Therefore, the current method for partitioning is a two-cycle approach that involves the separation of An(III) and Ln(III) together from HLLW in the first cycle, followed by lanthanide-actinide separation in the second cycle.

Group separation – O Φ CMPO

Several reagents have been proposed for the co-extraction of An(III) and Ln(III) from HLLW and a number of flow-sheets based on those reagents have been developed. The chemical structures of the extractants developed at chemistry group are shown in figure 1. Among the various reagents scrutinized, the octyl(phenyl)-*N,N*-diisobutyl carbamoylmethylphosphine oxide (O Φ CMPO) has been chosen for demonstration of minor actinide partitioning. This is due to the fact that O Φ CMPO system has been well studied over two decades worldwide and at IGCAR. For partitioning studies, a typical High Active Waste (HAW) solution arising from the reprocessing of the FBTR fuel irradiated to a burn-up of 155GWd/Te was characterized by various analytical techniques. Subsequently, a number of studies were carried out with this HAW using a TRUEX solvent phase composed of 0.2 M O Φ CMPO - 1.2

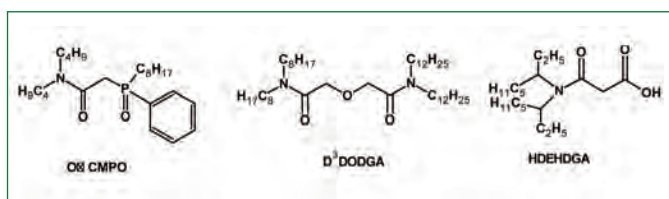


Figure 1: Structures of extractants developed at Chemistry Group, IGCAR

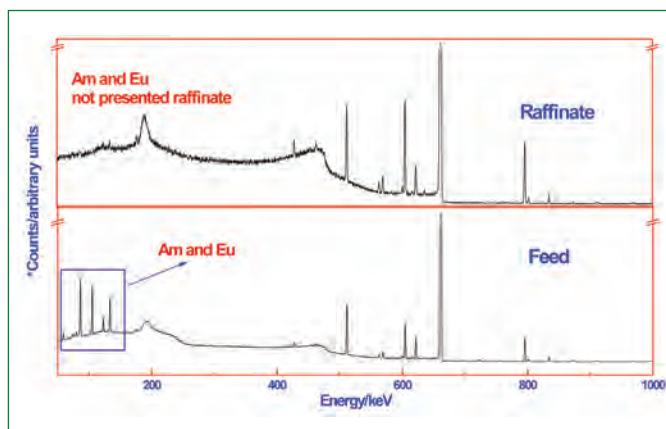


Figure 2: Gamma spectra of the feed and aqueous raffinate

M TBP in *n*-dodecane. A procedure was developed for quantitative separation of trivalent metal ions from HLLW and a new stripping formulation composed of 0.1 M citric acid in 0.1 M nitric acid was developed for the recovery of the metal ions from loaded organic phase. Based on these studies, partitioning of minor actinides from fast reactor dissolver solution was demonstrated. Figure 2 shows the gamma spectra of feed and aqueous raffinate which was obtained after the extraction run. The results confirmed near quantitative separation (> 99.9%) and recovery (>99%) of trivalents (Am+Ln) from high active waste.

Lanthanide – Actinide separation

The product stream obtained after minor actinide partitioning is composed of 0.1 M citric acid in 0.1 M nitric acid solution containing all trivalent actinides and lanthanides. Mutual separation of Ln(III) and An(III) was necessary as Ln(III) acts as neutron poison. Several ligands containing incinerable CHON atoms and also soluble in nuclear diluent, *n*-DD, have been developed for Ln-An separation. Among the various extractants scrutinized bis(2-ethylhexyl)diglycolamic acid (HDEHDGA, figure 1) was identified as promising extractant for mutual separation. Based on several trial studies with simulated wastes, the CMPO product stream obtained after minor actinide partitioning (155 GWd/Te) was treated for lanthanide-actinide separation using a 16- stage mixer-settler installed in hot-cell. The results established quantitative extraction of Am(III) and Eu(III) in 0.1 M HDEHDGA/*n*-DD in 1-2 stages. The organic phase was collected and subjected to stripping, using a solution composed of 0.01 M diethylene triamine penta acetic acid (DTPA) + 0.025 M CA at pH 1.5. The results demonstrate the possibility of separating actinides from lanthanides using HDEHDGA. It is worthwhile to mention here that the studies were demonstrated for the first time with a CHON based ligand, soluble in nuclear diluents, *n*-DD, for Ln-An separation and with the waste coming from the dissolver solution of FBR fuel solution.

Unsymmetrical Diglycolamides

In the previous decade, diglycolamides (DGAs) (alkyl-3-oxapentane-1,5-diamide derivatives) have emerged as promising candidates for partitioning of trivalent actinides from HLLW. The main drawback of the symmetrical octyl derivatives is the third phase formation and extraction of unwanted metal ions. To overcome the drawbacks, several unsymmetrical diglycolamides (UDGAs) have been synthesised and studied for the extraction of actinides and fission products from nitric acid medium. The results have shown that the dodecyl group in conjunction with the octyl group present in the UDGA, N,N,-didodecyl-N',N'-dioctyl-3-oxapentane-1,5-diamide, (D³DODGA, figure 1), not only retained the excellent extraction properties of octyl derivative of diglycolamides, but also surmounted the problem of third phase formation during the extraction of trivalent metal ions from 3-4 M nitric acid medium. The studies have also shown that D³DODGA does not require any phase modifier during the extraction of trivalent actinides from 3-4 M nitric acid medium.

Using D³DODGA, the extraction behavior of various metal ions present in the simulated high level liquid waste of fast reactor fuel solution that contained about 3.2 g/L of trivalent metal ions (Am(III) and Ln(III)) was studied in a solution of 0.1 M D³DODGA/n-DD. The co-extraction of unwanted metal ions was minimized by adding trans-1,2-diaminocyclohexane-N,N,N',N'-tetra-acetic acid (CyDTA), which was identified based on the studies undertaken in our laboratory as an appropriate reagent for preventing the extraction of unwanted zirconium and palladium. Based on several trial studies, a counter-current mixer-settler run was performed in a 20-stage mixer-settler. The quantitative extraction of Eu(III) and Am(III) was achieved in 7-8 stages. A counter current stripping run was performed using the same mixer-settler in a separate run. The study revealed that significant amount of trivalents were back extracted into the aqueous phase in the first contact itself, and all the trivalent metal ions were quantitatively back extracted into aqueous phase in 5 stages.

Based on this study, a flow-sheet shown in figure 3 could be proposed for the separation of trivalent metal ions. It can be seen that the flow-sheet is simple as compared to other flow-sheets developed for trivalent actinide partitioning. It requires 20 stages for quantitative extraction of trivalents and 3-5 stages for stripping. It is important to note that this method does not demand any scrubbing stages before stripping. The study also indicated that the problems due to crud formation or precipitation was not observed during the entire run, thus confirming the clean separation of trivalent metal ions demonstrating the advantage of D³DODGA for the separation of Am(III) from HLLW.

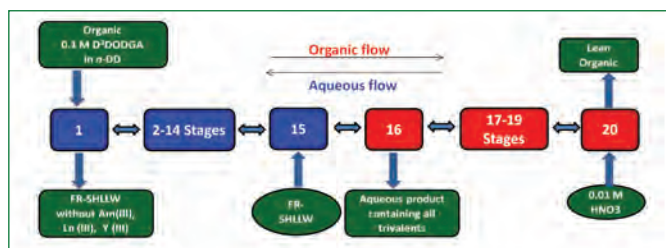


Figure 3: Flow-sheet for modifier-free minor actinide partitioning

SMART approach

Since D³DODGA offered several advantages as indicated above, a novel approach namely, Single cycle method for Minor Actinide partitioning using completely incinerable Reagents (SMART) has been explored which involves the coextraction of An(III) and Ln(III) together in the solvent phase followed by selective stripping of An(III) from the loaded organic phase. Acidic extractant HDEHDGA in conjunction with D³DODGA was chosen for the development of SMART procedure.

The distribution ratio of various metal ions present in FR-SHLLW was measured in a solution of 0.1 M D³DODGA + 0.2 M HDEHDGA/n-DD and the conditions needed for efficient extraction and selective stripping were optimized. The mixer-settler profiles showed that Am(III) and Ln(III) extraction occurred in 8-10 stages. The troublesome metal ions such as Zr(IV), Mo(VI), Fe(III), Cr(VI), Ni(II), Pd(II), Ru(III), Rh(III) were rejected to raffinate in addition to other elements. The recovery of Am(III) from the loaded organic phase was carried out using an aqueous formulation, 0.01 M DTPA + 0.5 M CA at pH 1.5. About 55% of the Am(III) was recovered after 20 stages (product stream). It was also observed that significant amount of early-lanthanides (from lanthanum to samarium) are stripped to the aqueous phase along with Am(III), whereas the later-lanthanides (beyond samarium) behaved similar to Eu(III) that remained in organic phase. The study clearly showed that the recovery of Am(III) was accompanied by the stripping of "lighter lanthanides". Therefore, the studies foresee the possibility of intra-lanthanides as well as lanthanide-actinide separation in a single-processing cycle.

In summary a flow-sheet was made available for partitioning of minor actinides from fast reactor high-active waste solution coming out of the dissolver solution of the fast reactor fuel of high burn-up (155 GWd/Te) by using a TRUEX solvent. Superior unsymmetrical diglycolamides were developed and a simple modifier-free flow-sheet based on D³DODGA was developed for group separation from FR-SHLLW. Using the combined CHON extractants, D³DODGA and HDEHDGA, a single-cycle approach was demonstrated for the separation of Am(III) alone from FR-SHLLW.

Reported by
K. A. Venkatesan and colleagues, Fuel Chemistry Division,
Chemistry Group

Young Officer's FORUM

A Spectral Energy Density Based Method to Understand The Temperature Dependent Phonon Frequencies In Materials

Knowledge of vibrations of the atoms in the crystal is crucial for understanding a wide range of physical properties of solids, such as specific heat, thermal expansion, thermal conductivity and phase transitions. The collective motion of atoms in solid forms a travelling wave called lattice vibrations. Phonons are the quanta of these lattice vibrations.

Lattice dynamics (LD) is the study of vibrations of atoms in crystals. In conventional lattice dynamics method, the phonon frequencies are obtained from the second derivative of inter-atomic potential under harmonic approximation; (the effects of anharmonicity are completely ignored). The finite temperature properties are modelled using the tedious quasi-harmonic approximation (QHA). The QHA works well up to intermediate temperatures and it is not suitable at high temperatures because of the phonon-phonon interactions, which are not directly included in QHA. The anharmonic effects have been studied using anharmonic lattice dynamics which employs empirical potentials as well as ab-initio calculations in conjunction with density functional perturbation theory (DFPT). In anharmonic lattice dynamics, the higher order phonon effects are neglected by truncating the crystal lattice potential energy at third order in the displacement of atoms from their equilibrium position.



Shri Anees. P obtained his M.Sc. in Physics from University of Calicut, Kerala. He is from 4th batch of BARC Training School at IGCAR campus. Presently he is a scientific officer in Materials Science Group. His current area of research is modelling thermal and phonon transport properties of materials using density functional theory (DFT) and molecular dynamics simulations.

Moreover, since we can handle at most only a few hundreds of atoms in DFPT, it will be difficult to model system size dependence of phonon transport. Since molecular dynamics (MD) simulations incorporate the anharmonicity of the inter-atomic potential without truncating it and also because it can handle systems having millions of atoms, it will be a natural choice to model the high temperature phonon properties of materials. In order to study the temperature dependence of the frequencies, dispersion and coupling of normal modes of vibration of a crystal, a spectral energy density based formalism has been developed. The contributions of phonon-phonon coupling and thermal expansion to the temperature dependence of all the phonon modes can be delineated by studying the phonon related properties of the very same system simulated in accordance with both canonical (NVT) and isobaric-isothermal (NPT) ensembles.

LD calculations are done to obtain the frequencies and polarizations of the normal modes of vibration of a perfect crystal within the harmonic approximation. Velocity of the atoms is obtained as a function of time from MD simulations. These velocities are projected on to the normal modes of vibration of the perfect crystal, and the phonon frequencies are obtained from its Fourier transform. This

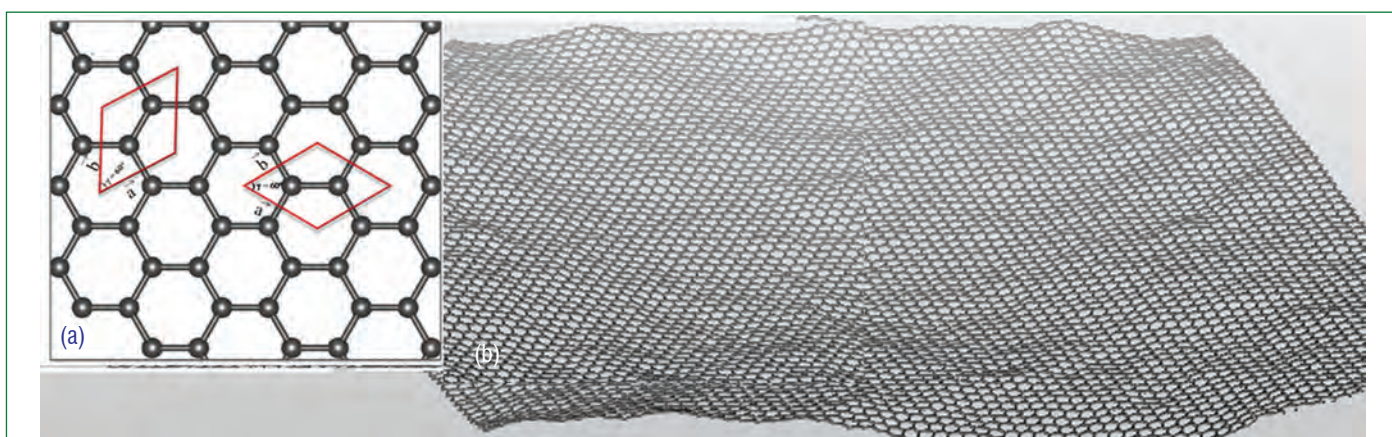


Figure 1: (a) 2D-unit cell of graphene (b) graphene sheet at 300 K with corrugations due to the thermally excited ripples. Such corrugations are seen in the simulations carried out at all nonzero temperatures.

method has been validated with C and Si crystal. Since graphene is a strong anharmonic 2D crystal, we applied this method on graphene to study its high temperature phonon properties. All the simulations are performed using the classical MD simulation package LAMMPS. The interaction between the carbon atoms in the honeycomb lattice of graphene is modeled using the long range bond order potential (LCBOP).

The 2D unit cell of graphene is shown in Figure 1. The simulations are carried out in three dimensions with periodic boundary conditions along all the three directions. In order to ensure that the interaction of the graphene layer with its replicas is negligible an inter-planar vacuum separation of 12Å is provided between the layers. The classical MD simulations are done with a simulation cell of size 70x70x1 (9800 atoms).

The phonon dispersion of graphene is as shown in Figure 2. The red solid curve is obtained from LD and the black curve is computed using data from MD simulations at 300 K using spectral density method. The experimental data of graphene are shown as symbols. The LD frequencies match with previous calculations and the agreement with the experiments is satisfactory. The unit cell of graphene contains two basis atoms, and hence there are six modes in the phonon dispersion (three acoustic+three optic modes). The letters L and T represent the longitudinal and transverse polarizations. The symbol Z denotes the out-of-plane vibrations (bending modes). The acoustic and optic modes are labeled using symbols A and O respectively. The LA and TA modes show linear dispersion near the Γ point in contrast with the quadratic dispersion

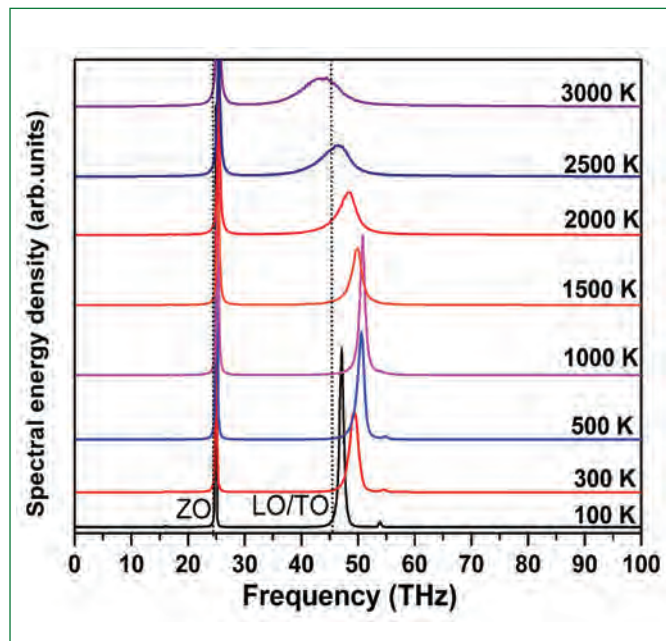


Figure 3: The ZO and LO/TO frequencies at Γ point as a function of temperature. The vertical lines (short dash) represent the peak positions of ZO and LO/TO frequency obtained from LD calculations

shown by the ZA modes, the latter being a characteristic feature of phonon dispersion of 2D layered materials. In the ZA mode the two atoms in the unit cell vibrate in-phase along the Z direction, and in the long wave length limit, this mode causes bending of the surfaces due to thermally excited ripples in the graphene sheets.

The temperature dependence of Γ point optic phonon modes is compared with Raman/IR data. In graphene, LD calculations using LCBOP potential predicts the peak position of degenerate longitudinal and transverse optic (LO/TO) modes at Γ point to be 45.38 THz at 0 K. From Figure 3 it is clear that as temperature increases the LO/TO mode frequency shows a blue shift. Similarly the ZO mode at 0 K peaks at 24.63 THz and shows a slight blue shift with temperature.

The shift in phonon frequency and change in phonon line width with temperature are due to the anharmonicity in the effective interaction between the atoms. Effect of anharmonicity can be separated into two parts: one that comes from the anharmonic coupling of phonon modes (self-energy change) and the other that arises from the thermal expansion/contraction of the crystal. Thermal expansion/contraction leads to the decrease/increase in the values of the force constants and hence a shift in the mode frequencies. On the other hand, the coupling between the phonon modes leads to finite lifetime (nonzero width) apart from a shift in the mode frequency. The phonon frequency shift with temperature that arises purely due to anharmonic coupling of phonon modes can be obtained from the constant volume simulations/experiments. Since most of

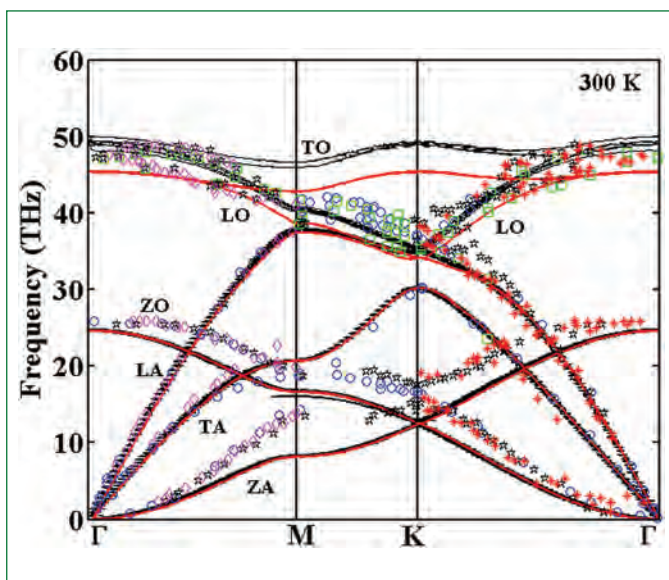


Figure 2: The phonon dispersion of graphene at 300 K. Upshift of phonon frequencies at 300 K (from MD) with respect to the 0 K frequencies (from LD) as well as a splitting of the ZO mode along M-K direction is conspicuous.

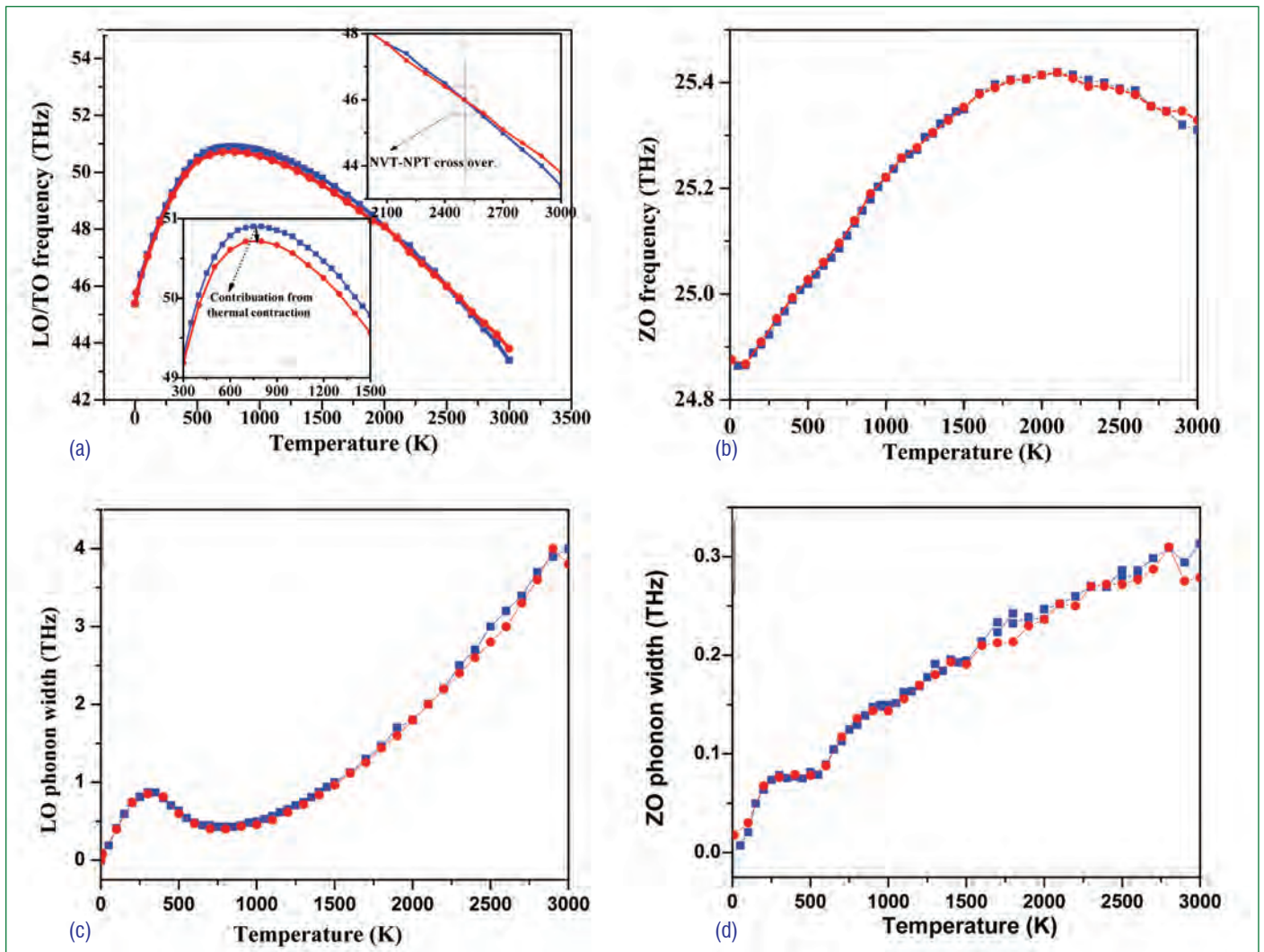


Figure 4: (a) LO/TO frequency shift with temperature. Enlarged view in the temperature range 300 - 1500 K shown in the inset depicts the contribution from in-plane thermal contraction. The inset in the temperature range 2000 - 3000 K shows the cross-over of NVT-NPT simulations (b) shift in ZO frequency with temperature. (c) & (d) phonon width as a function of temperature in NVT and NPT ensemble of LO/TO mode and ZO mode (-●- NPT ensemble, -■- NVT ensemble)

the experiments are performed at constant pressure, the observed frequency shift arises from the combination of thermal expansion and self-energy change. In the present work we decouple this self-energy change and thermal expansion contributions by performing constant volume (NVT ensemble) and constant pressure (NPT ensemble) simulations. Figures 4a&b show the shift in LO/TO and ZO frequency with temperature in NVT and NPT ensembles. It can be seen that the LO/TO frequency shows an upshift in both NVT and NPT simulation until ~ 2500 K beyond which a cross over occurs. The upshift in phonon frequencies in NVT ensemble is purely due to self-energy change, while upshift in NPT ensemble is a combination of self-energy change + thermal contraction of in-plane lattice. So both self-energy and thermal contraction are causing an up-shift in frequency. The LO/TO modes corresponds to in-plane atomic displacement, hence the behavior of LO/TO modes with temperature can be correlated with in-plane lattice thermal contraction/expansion behavior. The cross-over in

NPT and NVT ensemble at 2500 K implies that the lattice contraction occurs in graphene until ~ 2500 K and it expands afterwards.

On the experimental front, a redshift of the G-peak (E_{2g} mode or LO/TO mode) is seen in the temperature dependent Raman spectra of graphene sheets. The ab initio MD simulations carried out in the temperature range 0-2000 K show thermal contraction of free-standing graphene for various system sizes and the present results are consistent with these results. On the other hand, thermal expansion occurs for supported graphene sheets in the entire temperature range of simulation, and this might be the reason for the red shift seen in the experiments. In support of this argument, there are previous reports, that the in-plane lattice parameter of graphene over TaC (111) substrate is 3 % larger than the bulk graphite, which leads to a considerable softening of zone-centre optical phonons. The strong coupling between the graphene and substrate causes an increase in the in-plane lattice parameter

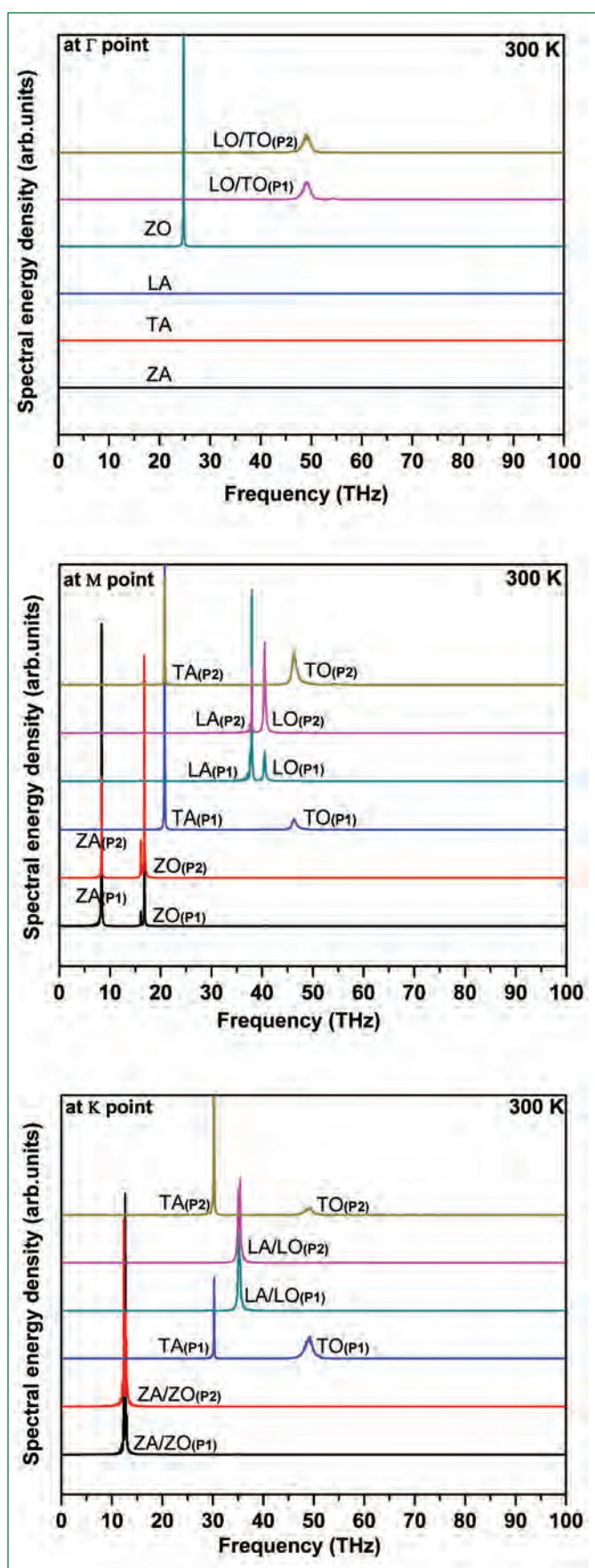


Figure 5: Spectral density is shown at some special points in the Brillouin zone to obtain information about anharmonic coupling and decay of each of the six phonon modes, where P1 and P2 are two different polarization

($\sim 3\%$), which is large enough to suppress the temperature induced contraction and its effect on phonon frequency shift.

In graphene the ZO mode is inactive in both Raman and IR scattering experiments. Figure 4b shows the variation of ZO mode frequency with temperature. The ZO mode frequency shows a maximum at ~ 2078 K. Both the NVT and NPT ensemble simulations predict the same shift in frequency in the entire temperature range; which indicates that the ZO mode frequency shift comes entirely from the anharmonic phonon coupling (self-energy change). The contribution from the thermal expansion is negligible. The phonon width is computed by fitting a Lorentzian to the frequency spread. Figure 4c&d show the width of LO/TO and ZO phonon modes at Γ point as a function of temperature. The width of the LO/TO phonons increases with temperature in a non-monotonic manner. The linewidth of ZO mode increases with temperature and the broadening is less when compared to LO/TO mode. Since ZO mode is inactive in Raman and IR scattering experiments, no experimental results are available for comparison.

Figure 5 shows the temperature dependent phonon spectra at 300 K at Γ , M and K points. The modes are designated as longitudinal or transverse as per their polarization at the Γ point. The modes are, in general, neither longitudinal nor transverse, but of mixed character, when the propagation is along a general direction. LO/TO modes do not get coupled with the other modes at Γ ; implying that their decay occurs by coupling with phonons at other points in Brillouin zone. At M point, the TO mode coupled with low frequency TA mode, and similarly the LO mode gets coupled with LA mode. At K point, the ZA/ZO and LA/LO modes are not coupled with other modes, and the TO mode gets coupled with TA mode.

In summary, we have developed a spectral energy density based formalism to enumerate the temperature dependence of the phonon frequencies, dispersion and coupling of normal modes of vibration in a crystal by carrying out two sets of calculations. First we carry out lattice dynamics calculations to obtain the frequencies and polarizations of the normal modes of vibration of the perfect crystal within the harmonic approximation, and then use molecular dynamics simulations to obtain the velocities of all the atoms in the system maintained at a fixed temperature as a function of time. Spectral energy density can then be obtained by taking the Fourier transform of the projection of these velocities to the polarization vectors of the normal modes of the perfect crystal. Unlike the conventional lattice dynamical methods, this methodology enables us to obtain the true anharmonic behavior of the materials.

Reported by

P. Anees, Materials Physics Division, Materials Science Group

Young Researcher's FORUM

Phase Transformations and Microstructural Evolution in 9Cr Reduced Activation Ferritic / Martensitic steels

9Cr-Reduced Activation Ferritic / Martensitic (RAFM) steels, are candidate structural materials for the test blanket module (TBM) of the International Thermonuclear Experimental Reactor (ITER), due to their excellent resistance to radiation-induced swelling, He embrittlement and acceptable high temperature mechanical properties. These steels have been developed by replacement of Mo and Nb by W and Ta respectively in a modified 9Cr-1Mo steel (P91) to minimise the level of induced radioactivity. The indigenous effort involved optimisation of composition and processing window, developmental and industrial scale production of the steels, evaluation of property and structure – property correlations which has led to the development of India specific RAFM (INRAFM) steel with 1.4W-0.06Ta for the Indian TBM. As a part of this effort extensive studies on the phase transformation characteristics and microstructural evolution of 9Cr RAFM steels with varying W (1, 1.4 and 2wt.%) and Ta from (0.06 and 0.14wt.%) have been



Dr. Ravikiran did his Masters in Materials Science from Mangalore University, Mangalagangothri, Mangalore. He joined IGCAR as a Junior Research Fellow in Engineering Science in August 2009 and carried out his doctoral work in the Physical Metallurgy

Group, MMG, under the guidance of Dr. Saroja Saibaba. His doctoral thesis was on “Study of transformation characteristics and microstructural evolution in 9Cr Reduced Activation Ferritic / Martensitic steel using electron microscopy, calorimetry and computational methods” He obtained the Ph.D degree from Homi Bhabha National Institute in February 2015. He is currently a Project Associate at IIT Madras.

carried out, the highlights of which are described in this article.

Phase transformation in RAFM steels – Role of W and Ta

The role of W and Ta on the mechanism and kinetics of phase transformation in RAFM steels have been studied by Differential Scanning Calorimetry (DSC) employing different heating and cooling rates. For a typical slow heating rate (3 K min⁻¹) the following sequence of transformations were established–

α -Ferrite (ferromagnetic) + M₂₃C₆ + MX → γ -ferrite (paramagnetic) + M₂₃C₆ + MX → γ -austenite + M₂₃C₆ + MX → γ + MX → γ + δ + γ → γ + δ + L → δ + L → Liquid.

The transformation temperatures A_{c1} and A_{c3} evaluated for the four steels are listed in Table 1. A_{c1}, A_{c3} did not show significant variation, while the solidus temperature of the steels showed an

Table 1: Transformation temperatures of RAFM steels at a heating rate of 3 K min⁻¹

Phase change	Transformation Temperature (K)			
	1W-0.06Ta	1.4W-0.06Ta	2W-0.06Ta	1W-0.14Ta
α' (Martensite) → α + M ₂₃ C ₆	937 ± 5	918 ± 5	917 ± 7	919 ± 4
TC, Curie temperature	1018 ± 5	1027 ± 5	1025 ± 5	1024 ± 5
α + MX + M ₂₃ C ₆ → α + γ + MX + M ₂₃ C ₆ (A _{c1} – onset of austenite)	1104 ± 5	1091 ± 5	1108 ± 5	1086 ± 5
α + γ + MX + M ₂₃ C ₆ → γ + MX + M ₂₃ C ₆ (A _{c3} – completion of austenite formation)	1144 ± 5	1130 ± 5	1135 ± 5	1114 ± 5
γ + MX + M ₂₃ C ₆ → γ + MX (M ₂₃ C ₆ dissolution)	1350 ± 5	1342 ± 10	1342 ± 10	Not clearly detected
γ + MX → δ + γ + MX (δ -ferrite formation)	1575 ± 5	1494 ± 10	1499 ± 10	1495 ± 10
δ + γ + MX → δ + γ (MX dissolution)	1581 ± 15	1563 ± 15	1570 ± 15	1565 ± 15
δ + γ → Liquid + γ + δ (solidus)	1730 ± 15	1762 ± 15	1788 ± 15	1784 ± 15
Liquid + γ + δ → Liquid + δ	1753 ± 15	1767 ± 15	1791 ± 15	1792 ± 15
Liquid + δ → Liquid (liquidus)	1805 ± 15	1791 ± 15	1794 ± 15	1796 ± 15

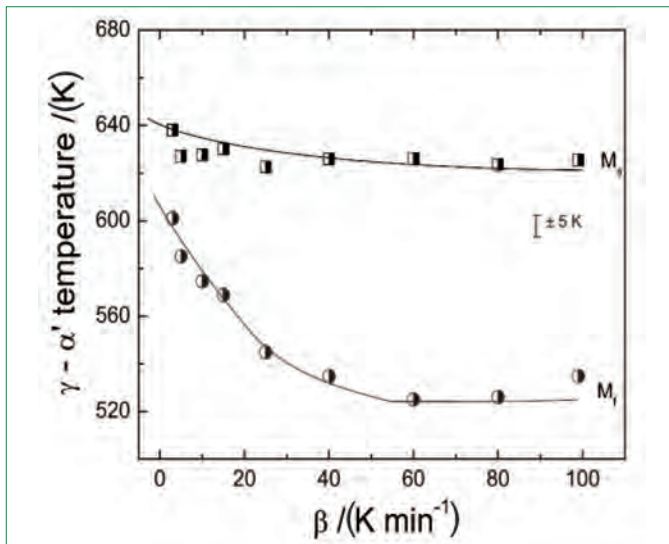


Figure 1: Cooling rate dependence of M_s and M_f temperatures

increase with the addition of refractory elements, W and Ta. The phase fraction and transformation temperatures of different phases in 1.4W-0.06Ta steel calculated using JMatPro® was also found to be in agreement with experimental results.

It is observed that the dissolution temperature of the carbides is well above A_{c3}, which influenced the kinetics of $\alpha \rightarrow \gamma$ transformation as evidenced by the increase in A_{c1}, A_{c3} with heating rate in 1.4W-0.06Ta steel due to the sluggish dissolution of the carbides. The reverse $\gamma \rightarrow \alpha / \alpha'$ transformation was also found to be dependent on the cooling rate. From Figure 1 it is observed that the martensite start temperature, M_s does not show considerable variation with cooling rate, while the finish temperature M_f shows a nonlinear variation below 40 K min⁻¹. Such a nonlinear dependence of M_f below 6 K min⁻¹ was found to be due to the diffusional transformation forming proeutectoid ferrite preceding the martensitic transformation, while a fully martensitic structure was obtained for cooling rates above 40 K min⁻¹. Hence the critical cooling rate for $\gamma \rightarrow \alpha'$ transformation is identified to be > 40 K min⁻¹. Further, M_s and M_f showed decrease with W and Ta content of the steel, which also agreed with values computed using empirical relationships.

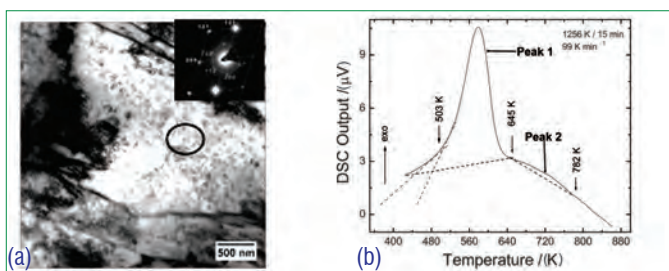


Figure 2: (a) TEM micrograph of normalised 1.4W-0.06Ta steel (b) DSC profile of the steel cooled at 99 K min⁻¹ from 1256 K with peaks corresponding to martensite transformation and pre-martensitic precipitation

Decomposition modes of austenite

It is well known that the decomposition mode of high temperature γ is dictated by alloy composition and cooling rate. Austenitisation at 1323 and 1253 K followed by air cooling showed a martensitic microstructure in all the steels, while furnace cooling led to a mixture of $\alpha + \alpha'$. However, detailed TEM studies showed the precipitation of fine, acicular Fe rich M₃C or M₂₃C₆ carbides within a few wide martensitic laths in 1.4W-0.06Ta and 2W-0.06Ta steels (Figure 2a), depending on the austenitisation temperature and cooling rate. This observation is rather unexpected, in 9Cr steels, which are air hardenable. A DSC thermogram for 1.4W-0.06Ta steel under similar cooling conditions is shown in Figure 2b. The major exothermic peak indicates the martensitic transformation, while the broad, small peak in the higher temperature regime was unambiguously confirmed to be due to M₃C precipitation above M_s, and not due to autotempering, which can take place only between M_s and M_f. This was further supported by TEM analysis of the post DSC sample. Such a precipitation of M₃C or M₂₃C₆ prior to martensitic transformation is attributed to the compositional inhomogeneity of γ due to the undissolved carbides during austenitisation. The solute lean austenite in the vicinity of undissolved carbides transform to $\alpha +$ carbides above M_s temperature, while solute rich γ away from the undissolved carbides transforms to α' .

Another interesting manifestation of the above mentioned inhomogeneity of γ was the presence of low amount of retained γ in a martensitic matrix, which was detected by Synchrotron XRD and Mossbauer spectroscopy and not by conventional TEM on normalised steel. However, Orientation imaging microscopy in TEM showed the retained austenite along with different orientations of the martensite laths (Figure 3(a)), while the phase map unambiguously confirmed the same (Figure 3(b)). Hence, an understanding of the role of tungsten and tantalum, in controlling the homogeneity of composition of the austenite is important for the optimisation of processing and heat treatment conditions for the RAFM steels, especially in thick sections or during repair welding of weldments.

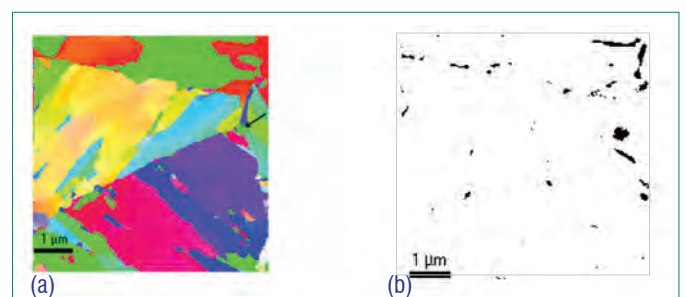


Figure 3: (a) Orientation imaging of normalised 1.4W-0.06Ta steel showing different orientation of martensite laths, (b) phase map showing retained γ

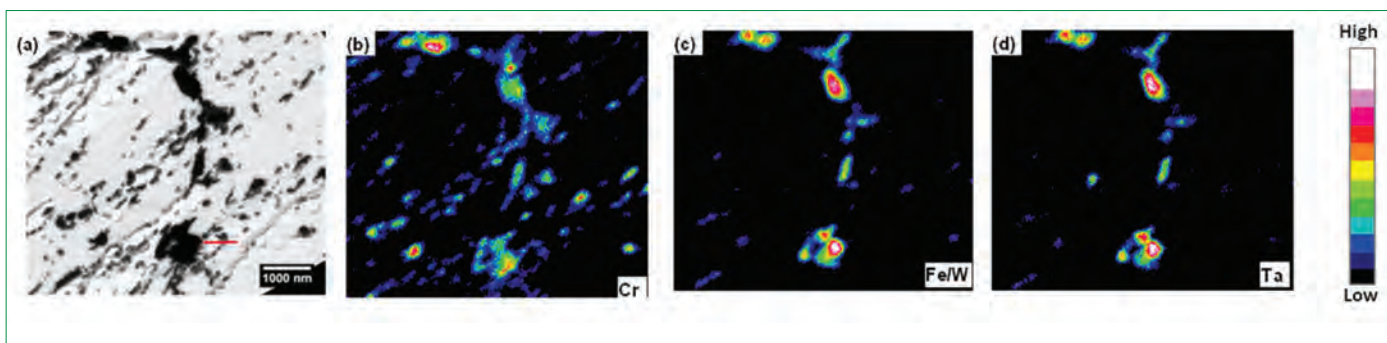


Figure 4: (a) Extraction replica micrograph of 2W-0.06Ta steel aged at 923 K for 5000h, (b-d) elemental mapping showing an enrichment of W and Fe in Laves phase

Microstructural evolution on aging

Prolonged thermal exposure of RAFM steels in the temperature range of 773-823 K showed a decrease in hardness, which is attributed to the softening of the matrix due to the depletion of solute elements through the coarsening of $M_{23}C_6$ carbides. In contrast, the 1W-0.06Ta steel showed a secondary hardening behaviour, after two hours of thermal exposure at 873 K, due to fresh nucleation of fine (20-40 nm) V and Ta rich MX precipitates. Further, hardness at 873 K was always higher than at lower temperatures, suggesting that these fine MX precipitates did not coarsen during aging and are effective in retarding the recovery of martensitic structure. On the other hand $M_{23}C_6$ carbides showed considerable coarsening up to 150-200 nm. However, the replacement of W in RAFM steel retards the coarsening of $M_{23}C_6$ precipitates as compared to P91/T91 steel. Hence, the substructural recovery is sluggish due to

the effective pinning of subgrain boundaries, which are responsible for the microstructural stability of the RAFM steels over prolonged exposure to high temperatures until 923 K. However, in steels with higher W and Ta content the formation of Laves phase was observed, which coarsened rapidly, leading to microstructural instability at temperatures exceeding ~ 900 K. X-ray map of the 2% W steel aged for 10000 hours at 923 K in Figures 4(a-d) shows the presence of coarse Laves phase, enriched with Fe and W, with limited solubility for Cr and Ta. Detailed analysis revealed that the Laves phase nucleates around the $M_{23}C_6$, while further coarsening of Laves phase and $M_{23}C_6$ is accompanied by the exchange of Cr and W at the Laves phase / $M_{23}C_6$ interface. The increase in Ta to produced a similar effect.

The prediction of secondary phases using JMatpro computations (Figure 5) in 1.4W-0.06Ta steel showed the formation of unstable carbides like M_3C , M_2X and M_7C_3 at short duration of less than 1 hour, while $M_{23}C_6$ and MX are predicted to be stable phases at 923 K. Nucleation of Laves and Z phase are also predicted after long durations. The absence of Z-phase in the present experimental study is attributed to kinetic factors. This prediction has been useful to identify the temperature regime of processing and operation to avoid the formation of secondary phases detrimental to the high temperature mechanical properties of the steel. Thus, this study has elucidated the effect of W and Ta on the phase transformation and microstructural evolution in 9Cr RAFM steels, which were useful inputs for the optimisation of alloy composition and design of heat treatment conditions.

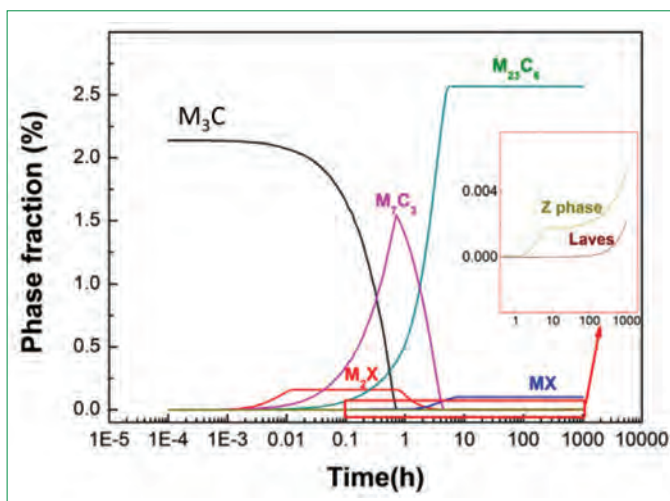


Figure 5. JMatPro simulation of secondary phase precipitation in 1.4W-0.06Ta steel aged at 923 K

*Reported by
Ravikiran, Microscopy and Thermo-Physical Property Division,
Metallurgy and Materials Group*

Diamond Jubilee Celebrations of the Department of Atomic Energy at Kalpakkam



Posters and Exhibits at Anu Vigyan 2015

Department of Atomic Energy established on 3rd August, 1954 has completed six decades of remarkable performance. Presently, we are commemorating the Diamond Jubilee of the Department. A series of lectures, exhibitions and visits to facilities at IGCAR for students from various colleges and educational institutions are being organized as a part of these celebrations. Some of the initiatives undertaken during the quarter, January-March, 2015 is highlighted below:

Participation in DAE Pavilion at the Science Congress in Mumbai University:

IGCAR took active part by putting up posters and exhibits at the DAE Pavilion during the Science Congress, Mumbai University premises in the month of January 2015.

ANU VIGYAN-Exhibition at Kalpakkam

Anu Vigyan a science exhibition at Kalpakkam Township, targeting

residents and neighbourhood was organized for two days during January 24-25, 2015. All the units of DAE at Kalpakkam have participated in the event by way of putting up an exhibition. The exhibition aimed at popularizing various activities of the Department, highlighted the role of DAE towards the well being of mankind, and also allayed the fear of radiation in the perception of the public. The exhibition also forayed into the myths in the minds of the public and informed the public about the benefits of nuclear energy. Impressive demonstrative models and illustrative posters attracted more than two thousand visitors including schools students and residents of the townships.

“Know your DAE” Lecture series:

During this quarter we had the lectures by eminent people giving a perspective of the Department to colleagues at Kalpakkam.

IANCAS(SRC) Radiochemistry workshop

In view of the diamond jubilee celebrations of DAE, IANCAS(SRC) Radiochemistry workshop was conducted at Meenakshi College, Chennai on 24 January 2015 (Saturday). Shri K. A. Venkatesan, Dr. T. G. Srinivasan, Dr. R. Kumar, Dr. N. Ramanathan and Shri G. V. S Ashok Kumar of IGCAR attended the workshop as resource persons. About hundred students from B.Sc.

S. NO	DATE	Delivered by
1.	February 24, 2015	Shri S.S. Bajaj Distinguished Scientist, Chairman AERB
2.	March 14, 2015	Dr. Baldev Raj Director, NIAS



Posters and Exhibits at Anu Vigyan 2015

Physics and Chemistry discipline participated in the workshop. The morning session comprised of two lectures, one on Fundamentals of Radiochemistry and the other on Applications of Radioisotopes were delivered by Dr. N Ramanathan and Dr. R Kumar. The afternoon session comprised of practical demonstrations aimed at determination of half-life of barium-137 m isotope, and half-value thickness of lead. The workshop was well received.

Outreach & Awareness Programmes

Several exhibitions were organized across Tamil Nadu by IGCAR.

These Exhibitions played a major role in educating the public about nuclear energy and the activities of DAE. It also helped in dispelling the fear about the activities of the department amongst them.

State-level Quiz and Painting Competitions:

A state-level Science Quiz and painting competition for arts and science colleges was conducted for UG & PG students of the colleges. Zone I covered the districts of Kanyakumari/ Nagercoil, Tirunelveli and Thoothukudi. Around 63 teams participated in the competition. It was organized successfully at Women's Christian College, Nagercoil during March 24-25, 2015.

SL NO	DATE	Event
1.	January 7-8, 2015	National Science Fair 2015 Organized by OMEIAT M.E.S.Razeena Matriculation Higher Secondary School, Chennai
2.	February 26-March 1, 2015	Chennai Science festival
3.	March 2-4, 2015	WAVES'2015 at Anna University, Chennai
4.	March 9, 2015	Nuclear Awareness for Rural public at Vadapattinam, Kancheepuram District

Conference and Meeting Highlights

Orientation Programme for Young Officers

February 16 – March 6, 2015



Dr. P.R. Vasudeva Rao, Director, IGCAR addressing the young officers during the valedictory function

Orientation Programme for the directly recruited young officers and officers from Training Schools other than IGCAR, who have joined our Department in the recent past, was organized during February 16 – March 6, 2015

This three week long programme, was designed to give an outline of the R&D activities of our Centre to the young officers. Each day a senior colleague from the DAE facilities delivered a lecture on the research activities of their Group and it was followed by a visit to the respective facility.

The officers were also informed about the activities of other DAE units located at Kalpakkam by senior colleagues of the respective Units. Visits were arranged to MAPS, BHAVINI and BARC-Facilities located at Kalpakkam.

Interactive sessions were also organized for bringing awareness about Administration, Accounts and Purchase procedures, Rules in Contributory Health Service Scheme and Industrial Safety Practices. Officers from BARC Training School, IGCAR joined in the recent past were also invited to participate in this interactive session.

The orientation programme concluded with a feedback session from the participants and with a address by Dr. P. R. Vasudeva Rao, Director, IGCAR as a part of the valedictory function.

*Reported by M. Sai Baba,
Associate Director, Resources Management Group*



Group photograph of participants with Dr. P.R. Vasudeva Rao, Director, IGCAR and colleagues of RMG during the valedictory function

Conference and Meeting Highlights

11th CEA-IGCAR Annual Meeting on Liquid Metal Fast Breeder Reactor Safety

March 23-27, 2015



Dr. P.R. Vasudeva Rao, Director, IGCAR welcoming the CEA delegates

IGCAR and CEA, France have worked together in the field of liquid metal fast breeder reactor safety. Under this bilateral cooperation, many collaborative projects have been taken up and completed. The 11th CEA-IGCAR annual meeting to review the ongoing collaborative project took place during March 23-27, 2015. The CEA team led by Dr. Christian Latge consisted of ten experts and the IGCAR team was led by Dr. P. R. Vasudeva Rao, Director IGCAR. During the meeting Implementing Agreements for collaboration on new projects

were also signed. Following ongoing collaborative projects among others were reviewed during the meeting.

- Fluid structure interaction applied to core mechanical behavior
- Carbonation of Na aerosols
- Atmospheric dispersion modeling
- Bench mark on Oxide (Phenix pin) and Carbide (FBTR Pin) Fuels Safety Criteria evaluation
- Testing of IGCAR ECHM on a sodium facility at Cadarache
- Experimental & theoretical studies for under sodium viewing for navigation and object detection
- Characterization of gas content in sodium
- Severe accident in sodium cooled fast reactor
- Dislocation precipitate interaction at high temperature in model ODS Alloys
- Thermodynamic Modeling of the actinide carbides and oxides systems
- Sodium Fast Reactor Education and Training



During the signing of agreement

*Reported by
B. K. Nashine, Reactor Design Group*

Visit of Dignitaries



Dr. R. Muralidharan, Director, Solid State Physics Laboratory, DRDO, New Delhi, delivering the IGC Colloquium

Dr. R. Muralidharan, Director, Solid State Physics lab, DRDO, New Delhi, delivered the IGC Colloquium on " Semiconductor Materials and Device Research and Development at Solid State Physics Laboratory an Overview ", during his visit to the Centre on January 06, 2015.



Dr. S. K. Malhotra, Head, Public Awareness Division, DAE, delivering the IGC Colloquium

Dr. S. K. Malhotra, Head, Public Awareness Division, DAE, delivered the IGC Colloquium on " Nuclear Power: The Need, Perception, and the Realities ", during his visit to the Centre on January 23, 2015.

Visit of Dignitaries



Prof. Ashok Jhunjunwala, Indian Institute of Technology, Madras, delivering the IGC Colloquium

Prof. Ashok Jhunjunwala, Department of Electrical Engineering, Indian Institute of Technology, Madras, delivered the IGC Colloquium on "Can India have Uninterrupted Power in all its Homes: Leveraging Decentralised Solar-DC", during his visit to the Centre on February 19, 2015.



Shri S.S. Bajaj, Chairman, AERB, delivering the Diamond Jubilee Colloquium

Shri S. S. Bajaj, Chairman, AERB, delivered the lecture on "Safety Regulation of Nuclear and Radiation Facilities in India", on February 24, 2015, as a part of "Know your DAE" series organized to commemorate the Diamond Jubilee Celebration.

Visit of Dignitaries



Dr. Baldev Raj, Director, National Institute for Advanced Studies, Bengaluru, delivering the Diamond Jubilee Colloquium

Dr. Baldev Raj, Director, National Institute for Advanced Studies, Bengaluru, delivered the lecture on "Energy Security and Sustainability: Approaches and Priorities for Growing and Aspiring India", on March 14, 2015, as a part of "know your DAE" series organized to commemorate the Diamond Jubilee Celebration.

Awards & Honours

Dr. P. R. Vasudeva Rao, Director, IGCAR has been selected as the **Vice President** for the Council of Materials Research Society of India

Dr. S. Amirthapandian has received the "Young Scientist Award" for the year 2014 from the Academy of Sciences, Chennai

Dr. John Philip has been elected as a member of the editorial committee for the Indian Journal of Engineering & Materials Sciences

Dr. N. R. Sanjay Kumar has received the Best Thesis award for his thesis titled "High Pressure High Temperature Synthesis and Study of Novel Transition Metal Carbides" during the 59th DAE Solid State Physics Symposium. The award is instituted by Indian Physics Association

Dr. N. V. Chandra Shekar has been selected by President, MRSI to receive the MRSI Medal for the year 2015

Best Paper/Poster

Ab-initio study of the Magnetism, Structure And Spin Dependent Electronic States of Ti substituted MO (M=Mg, Ca, Sr)

Dr. G. Jaiganesh and Dr. S. Mathi Jaya

59th DAE Solid State Physics Symposium

Best Poster Presentation Award

Patent

"Wash Solution Suitable for use in Continuous Reprocessing of Nuclear Fuel and a System Thereof"

authored by **Dr. P. Govindan, Shri K. Dhamodharan, Shri K. S. Vijayan, Dr. R. V. Subba Rao, Shri M. Venkataraman and Dr. R. Natarajan**, has been granted as patent by Japan - (Japanese Patent No. 5643745)



Bullet-wood tree

Dr. M. Sai Baba,

Chairman, Editorial Committee, IGC Newsletter

Editorial Committee Members: Dr. K. Ananthasivan, Shri M. S. Chandrasekar, Dr. N. V. Chandra Shekar, Dr. C. Mallika, Shri K. S. Narayanan, Shri V. Rajendran, Dr. Saroja Saibaba and Dr. Vidya Sundararajan